First-Layer Effect in Graphene-Enhanced Raman Scattering

*Xi Ling and Jin Zhang**

Graphene as a substrate for enhancing Raman scattering, called graphene-enhanced Raman scattering (GERS), has been reported in previous work. Herein, it is found that the "first-layer effect", which is widely used to explain the chemical-enhanced mechanism in surface-enhanced Raman scattering (SERS), exists in the GERS system. The Langmuir–Blodgett (LB) technique is used to construct mono- and multilayer ordered aggregates of protoporphyrin IX (PPP). Raman spectra of PPP with different layer numbers of the LB film on graphene are collected. The Raman signal from the first monolayer LB film of PPP has a larger contribution to the Raman enhancement than that from subsequent monolayers. Meanwhile, the Raman enhancement is dependent on the molecular configuration in contact with graphene, in which the functional group of PPP in direct contact with graphene has a stronger enhancement than other groups. These results reveal that GERS is strongly dependent on the distance between graphene and the molecule, which is convincing evidence that the Raman enhancement effect based on graphene belongs to the chemical-enhanced mechanism. This discovery provides a convenient system for the study of the chemical-enhanced mechanism and will benefit further understanding of SERS.

1. Introduction

Raman spectroscopy is an important tool to characterize the structure of materials. Specifically, the discovery of surface-enhanced Raman scattering (SERS) greatly promoted the development and application of Raman spectroscopy.[1–6] However, the mechanism of SERS is still a puzzle,[7–15] even though there are two widely accepted mechanisms: the electromagnetic mechanism (EM) and chemical mechanism (CM). The difficulty in understanding the mechanism of SERS is that the two mechanisms are always coexistent. Especially, the giant enhancement based on EM always covers the enhancement based on CM, which leads to a lot of difficulties in studying the CM.

To isolate the CM from the EM, most previous research employed a smooth metallic surface which was thought unable to support the EM enhancement.[12,13,16] However, a smooth metallic surface is not so easy to obtain. Usually, it was obtained by cold atomic deposition under an ultrahigh vacuum and low temperature.[12,13,16–21] Additionally, Raman spectra collection should be done in situ in an ultrahigh vacuum system to protect the surface. Hence, a convenient system, which supports only one mechanism, is needed and will benefit the study of SERS.

Graphene-enhanced Raman scattering (GERS) is a new technique in which graphene can be used as a substrate for enhancing Raman signals of adsorbed molecules.[22] Graphene is an ideal 2D structure with a monolayer of carbon atoms packed into a honeycomb crystal plane and it has several characters.[23] Firstly, it is relatively smooth in spite of fluctuations that follow from the underlying substrate.[24]

X. Ling, Prof. J. Zhang
Center for Nanochemistry
Beijing National Laboratory for Molecular Sciences
Key Laboratory for the Physics and Chemistry of Nanodevices
State Key Laboratory for Structural Chemistry of Unstable and Stable Species
College of Chemistry and Molecular Engineering
Peking University, Beijing 100871, P.R. China
E-mail: jinzhang@pku.edu.cn

DOI: 10.1002/smll.201000918

small NANO MICRO

Secondly, the optical transmission through the graphene surface in the visible range is more than 95%.[25] Finally, the surface plasmon on graphene is in the range of terahertz rather than the visible range.[26] Based on these considerations, graphene does not support the EM and it will be convenient to study the CM if the graphene-enhanced Raman effect observed in our previous work does indeed belong to the CM, as in our previous expectation. In fact, recently, stronger Raman enhancement was found in the metallic nanoparticle–graphene complex system when compared to the metallic nanoparticle-only system, even though no further explanation was given.[27]

One of the most important features of chemical enhancement is the short-range effect, in which the enhancement factor follows exponential decay as d^{10} (d is the distance between the probe molecule and the substrate).[12] This means that observable chemical enhancement can exist only when the probe molecule is close enough to the substrate. This feature was investigated by showing the existence of the "first-layer effect" in previous works.[12,13,16] The first-layer effect is a concept introduced by Moskovits in 1981,[28] who pointed out that the first absorbed layer, if bonded "chemically" to the metal, could couple to the surface plasmons through the periodic charge transfer that accompanies the adsorbate's vibration, which induced the Raman spectrum of the first monolayer that was especially enhanced over that of subsequent monolayers. However, during the 1980s to 1990s, this concept was developed by Otto, who pointed out that the first-layer effect was restricted to directly adsorbed molecules, which could not be understood within a classical electromagnetic enhancement mechanism.[13] After that, the first-layer effect was studied actively as evidence of the chemical-enhanced mechanism.[12,13,16,17] To demonstrate the first-layer effect, based on a surface with atomic-scale roughness obtained by cold deposition in the ultrahigh vacuum, the following designs have been mainly used: 1) the dependence of intensity on exposure, by showing the saturation of the intensity of the Raman signal after the first-layer deposition;[17] 2) spacer experiments, by showing the decrease or disappearance of the Raman signals after inserting a weak Raman scatterer between the substrate and the molecule;[13,29] 3) temperature-activated place exchange, by showing the appearance or enhancement of the Raman signals from the second-layer molecule after place exchange induced by heating;[12] and 4) oxygen quenching of the enhancement, by showing the decrease of the Raman signals after pre-exposure to oxygen for several minutes.[16] Anyway, all the results showed that the Raman enhancement based on the chemical-enhanced mechanism was prominent only when the molecule contacted the surface directly.

Based on the above discussion, GERS is an ideal system to avoid the EM. In the present study, to further confirm the CM in GERS, the Langmuir–Blodgett (LB) technique was used to construct mono- or multilayer ordered aggregates of protoporphyrin IX (PPP) and controllable molecular configurations of PPP in contact with graphene. Raman spectra were collected for different layer numbers and different molecular configurations of the LB film of PPP in contact with graphene. The results showed that the first-layer LB film of PPP, especially the chemical group closest to graphene, contributed the most to the Raman enhancement. It gave more convincing evidence showing that GERS obeyed the chemical-enhanced mechanism.

2. Results and Discussion

2.1. Construction of PPP–Graphene Complex Structures and Characterization

Figure 1 shows a schematic diagram of the process of sample preparation. Two typical structures were fabricated. For structure A, graphene was first transferred onto a clean SiO_2/Si substrate by mechanical exfoliation, and then the LB film of PPP was transferred onto it. In this structure, PPP is perpendicular on top of graphene with the hydrophilic group in contact with graphene. For structure B, with the opposite process, the LB film of PPP was transferred onto a clean SiO_2/Si substrate first, and then graphene was transferred onto it. In this structure, PPP is perpendicular on the bottom of graphene with the hydrophobic group in contact with graphene. It should be noted that multilayer LB films of PPP can also be fabricated by transferring a monolayer LB film more times.

Figure 2a shows the π–area (A) curve for the preparation of the monolayer LB film, in which the target pressure was controlled to 25 mN m^{-1}. The transfer ratio was near to 1 and only a few scratches were seen from the optical image. Atomic force microscopy (AFM) characterization also showed it was a perfect film, and the thickness was about 1.4 nm from the section analysis in a scratch (Figure 2b). The AFM images corresponding to the structures A and B are also shown in Figure 2c and d, respectively, from which we can see the perfect amalgamation of the film and graphene. It should be noted that there was little effect upon transferring

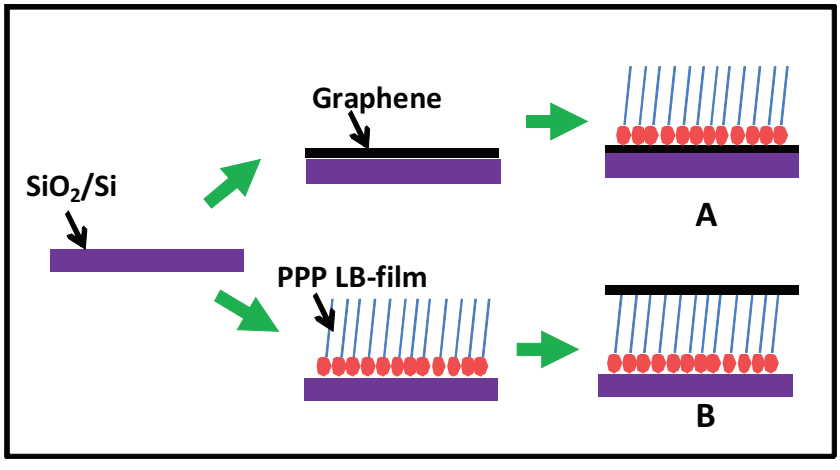

Figure 1. Schematic diagram of the sample preparation.

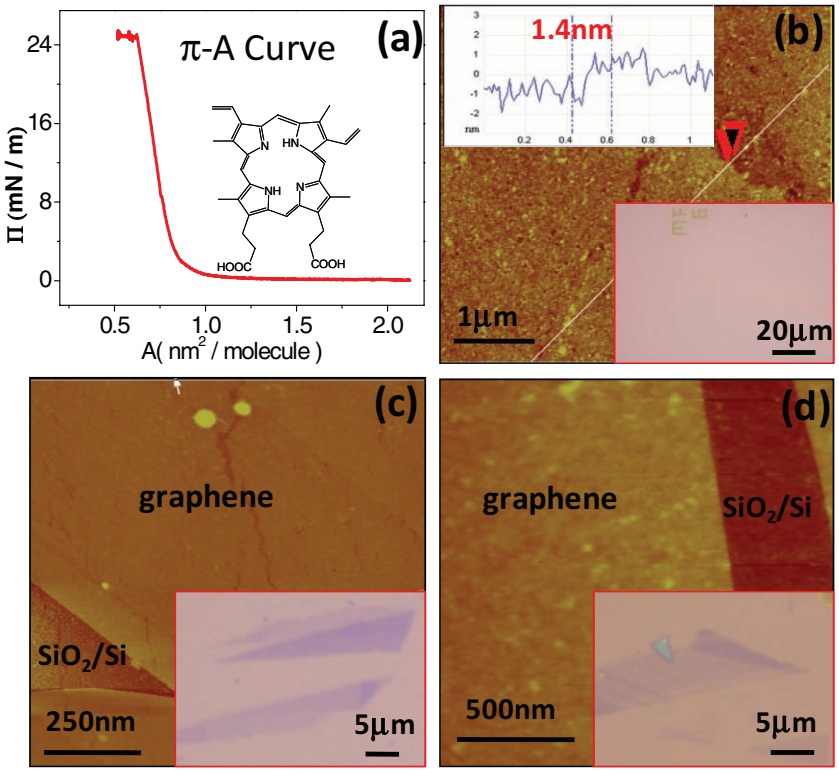

Figure 2. a) *π–A* curve of PPP. The inset shows the structure of PPP. b) AFM image of a LB film of PPP on a SiO_2/Si substrate. The top left inset shows the section analysis of the monolayer LB film. The bottom right inset shows the optical image of the monolayer LB film of PPP on a 300 nm SiO_2/Si substrate. c,d) AFM images of the monolayer LB film of PPP on the top (c) and bottom (d) of graphene. The insets show their respective optical images.

graphene after the introduction of the LB film of PPP for structure B, and no effect on the visibility of graphene by optical microscopy for both structures A and B (see the insets in Figure 2c,d).

The Raman enhancement effect has been reported to exist in a similar system with structure A in our previous work.[22] For structure B, where PPP was on the bottom of graphene, the Raman enhancement effect was also investigated. As before,[22] we compared the Raman signals from PPP collected on the SiO_2/Si substrate and on graphene. From **Figure 3**, it is obvious that the Raman signals from PPP collected on graphene are stronger than that on the SiO_2/Si substrate. This shows that the Raman enhancement effect existed on graphene even though the molecules were on the bottom.

2.2. Dependence of the Raman Enhancement on the Layer Number of the LB Film of PPP

Since the Raman enhancement effect exists in the GERS system no matter whether PPP is on the top or the bottom, we investigated the dependent relationship of the Raman enhancement on the layer number of the LB film of PPP for both situations. **Figure 4**a shows the Raman spectra of one to four layers of LB film of PPP on blank SiO_2/Si substrates. Even though the Raman signals from PPP are very weak because of no Raman enhancement, we can still confirm that the LB films are transferred onto the substrate successfully by the small differences between different layers from the peaks at 1360 and 1610 cm^{-1}. Then, graphene was transferred onto the above SiO_2/Si substrates with different layer numbers of the LB film of PPP. Figure 4c shows the Raman spectra collected on graphene with different layers of LB film of PPP on the bottom. Similarly, Figure 4b shows the Raman spectra collected on a piece of graphene with different layer numbers of LB film of PPP on top. From both Figure 4b and c, first, the Raman signals from PPP are much larger when compared with the blank in Figure 4a, which is consistent with the Raman enhancement effect on graphene. Besides, by comparing the Raman spectra from one to four layers of LB film of PPP with graphene on the top (Figure 4c) or the bottom (Figure 4b), we found that the change of the intensities of the Raman signals was very small even though the layer number of the LB film of PPP was increasing. Taking some peaks as references, such as 738, 1329, 1360, 1480, and 1610 cm^{-1}, Figure 4d shows the change of the relative Raman intensities as the LB film layers of PPP accumulated corresponding to Figure 4c, where the Raman scattering intensity from the monolayer LB film of PPP was set to "1". Clearly, the Raman intensities increase less and less after monolayer accumulation, thus indicating that the first layer of PPP plays an important role and contributes the most to the Raman enhancement.

The feature shown in Figure 4d is consistent with most of the reports about the first-layer effect.[16,18,20] It can be understood easily from the distance dependence of the charge transfer. As we know, charge transfer can result in the shift of the Raman

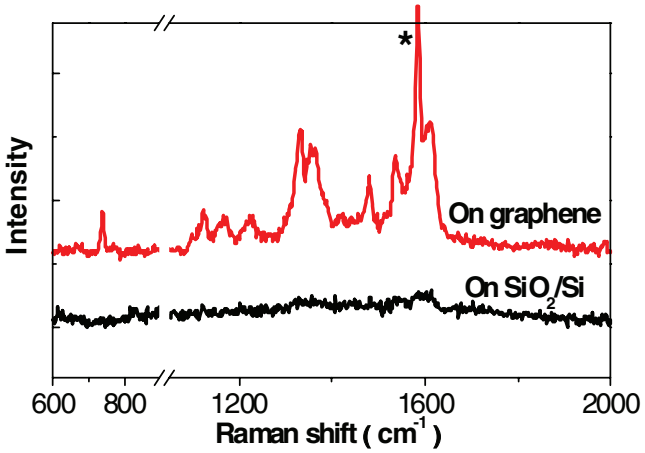

Figure 3. Comparison of the Raman spectra of a monolayer LB film of PPP on the SiO_2/Si substrate (black line) and on the bottom of a piece of graphene (red line). The peak labeled with "*" is the G-band from graphene.

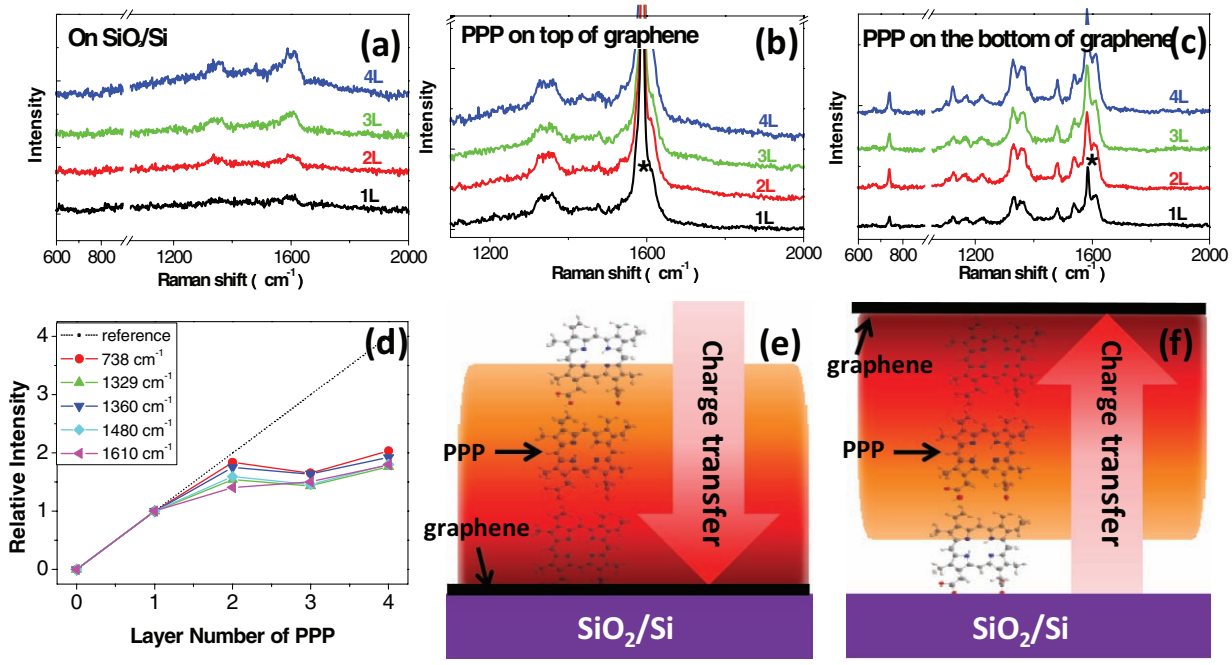

Figure 4. Raman spectra of PPP with different layer numbers of the LB film on a blank SiO_2/Si substrate (a), and on the top (b) and the bottom (c) of graphene. The peaks labeled with "*" are the G-band from graphene. d) Relative intensities of Raman signals from PPP corresponding to (c) as a function of the layer number of the LB film of PPP. The Raman signals corresponding to the monolayer LB film of PPP were set as "1". The lines with different colors correspond to the peaks labeled in the inset. The black dotted line is a reference considering that the different numbers of layers of PPP contribute equally. e,f) Schematic diagrams of the contribution of the different numbers of LB film layers of PPP to the charge transfer between graphene and PPP, corresponding to the situations in (b) and (c), respectively.

frequency.[30] **Figure 5** shows a comparison of the G-band of graphene before (black line) and after (red line) the deposition of PPP. Before deposition, the Raman shift of the G-band of graphene is at 1596 cm^{-1}, while it shifts to 1588 cm^{-1} after the deposition of PPP. This downshift can contribute to the charge transfer between graphene and PPP, where the electrons transfer from PPP to graphene. In fact, the shift of the Raman signals from PPP was expected by comparison with the Raman spectra of the PPP powder. However, there was only fluorescence background from the PPP powder, which made the Raman signals invisible (see Supporting Information, Part 1). Besides, from the change of the intensity of the G-band of graphene in Figure 5, it is clear that the Raman signal of graphene was also enhanced after the deposition of PPP. This can be understood by the interactional process of charge transfer. Charge transfer between graphene and PPP will not only enhance the Raman scattering cross section of PPP, but also that of graphene. It is also interesting to observe that the stronger the enhancement of the Raman signal of PPP is, the stronger the enhancement of that of graphene will be (see Supporting Information, Part 2). As we know, charge transfer usually occurs in a distance level below 1 nm, and decays quickly with the increase of the distance. Considering our system, PPP deposited by the LB technique stands up on the substrate, and the height of a PPP molecule is about 1.5 nm theoretically[31] and is about 1.4 nm in our experiment, as shown by the AFM section analysis in Figure 2b. Hence, charge transfer can only occur between the first-layer PPP molecule and graphene, and the contribution of the charge transfer from the second (or more) layer can be neglected, as shown schematically in Figure 4e and f, which correspond to the situations in Figure 4b and c. This result proved the existence of the first-layer effect directly, which is an important feature of the chemical-enhanced mechanism.

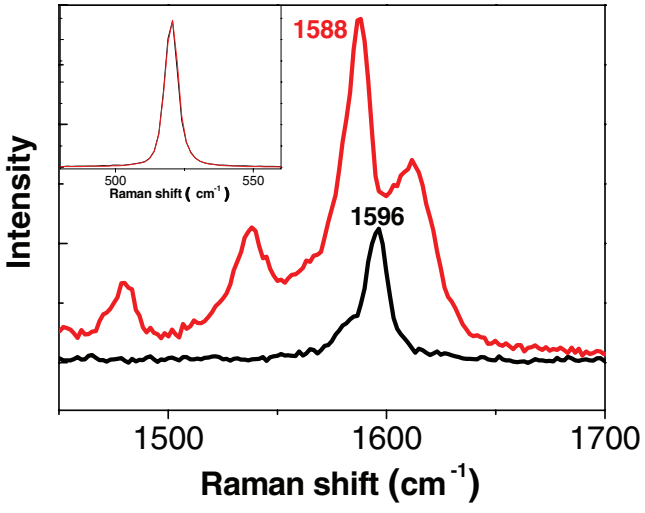

Figure 5. Comparison of the G-band of graphene before (black line) and after (red line) the deposition of PPP. The peaks labeled by number are the G-band of graphene, and other peaks are from PPP due to the Raman enhancement. The inset shows the corresponding peak at 520 cm^{-1} from silicon, which indicates the result of calibration of the position and intensity of the Raman signal.

Moreover, based on the distance dependence of charge transfer, a spacer layer was used to separate graphene and the LB film of PPP and thus prevent charge transfer between them. The spacer layer we used was a weak Raman scatterer, such as a monolayer LB film of arachidic acid (AA) or a thin layer of poly(methyl methacrylate) (PMMA). As expected, no Raman enhancement signals were observed. The data are shown in the Supporting Information, Part 3.

2.3. Dependence of the Raman Enhancement on the Molecular Configuration in Contact with Graphene

Furthermore, the dependent relationship of the Raman enhancement effect on the molecular configuration in contact with graphene was investigated. As mentioned before, for structures A and B, due to the opposite construction process, the molecular configuration (i.e., chemical group) in contact with graphene is different. For structure A, the functional group in contact with graphene directly is the hydrophilic group (–COOH; see the left inset of **Figure 6**a), while it is the hydrophobic group (–CH=CH_2) for structure B (see the right inset of Figure 6a). Raman spectra in these two situations were collected and compared in Figure 6a, and it is exciting to find that the Raman enhancement efficiency is quite different for these two structures, even though the number of PPP molecules is almost the same. The Raman signal we observed for the situation in structure B (blue line) is much stronger than that for the situation in structure A (red line). In fact, this phenomenon can also be observed by comparing Figure 4b and c. It should be noted that most of the Raman signals we observed, such as those at 738, 1123, 1164, 1220, 1330, 1360, 1480, 1537, and 1606 cm^{-1}, can be assigned to the vibrations related to the vinyl group or the porphyrin ring (see **Table 1**) as references.[32,33] The data showed that when the vinyl group was closer to graphene, the Raman signals were enhanced more (blue line in Figure 6a), and they were enhanced less if the vinyl group was far away from graphene (red line in Figure 6a). Hence, the phenomenon observed in Figure 6a is consistent with the distance dependence of the Raman enhancement mentioned in Section 2.2, which again indicates the chemical-enhanced mechanism in this system.

Furthermore, for comparison, copper(II) phthalocyanine (CuPc), which has a symmetrical molecular structure, was used to perform the same experiment. The construction of its LB film followed Reference [34]. Figure 6b shows a comparison of the Raman spectra of CuPc on the top (red line) and the bottom (blue line) of graphene. It was found that the intensities of the Raman signals were almost the same for both situations, which was very different from what we observed in Figure 6a where PPP was used. It shows that if the molecule is symmetrical, no matter which situation, the configuration in contact with graphene is the same, which results in equal Raman enhancement for both structures A and B.

The dependent relationship of the Raman enhancement effect on the molecular configuration showed that the vibrations related to the chemical group in direct contact with graphene had a stronger enhancement, which can also contribute to the distance dependence of the charge transfer. The closer the chemical group is to graphene, the larger the degree of charge transfer between them will be, which will induce a larger polarizability tensor of the vibrations and then a larger Raman scattering cross section for this chemical group.

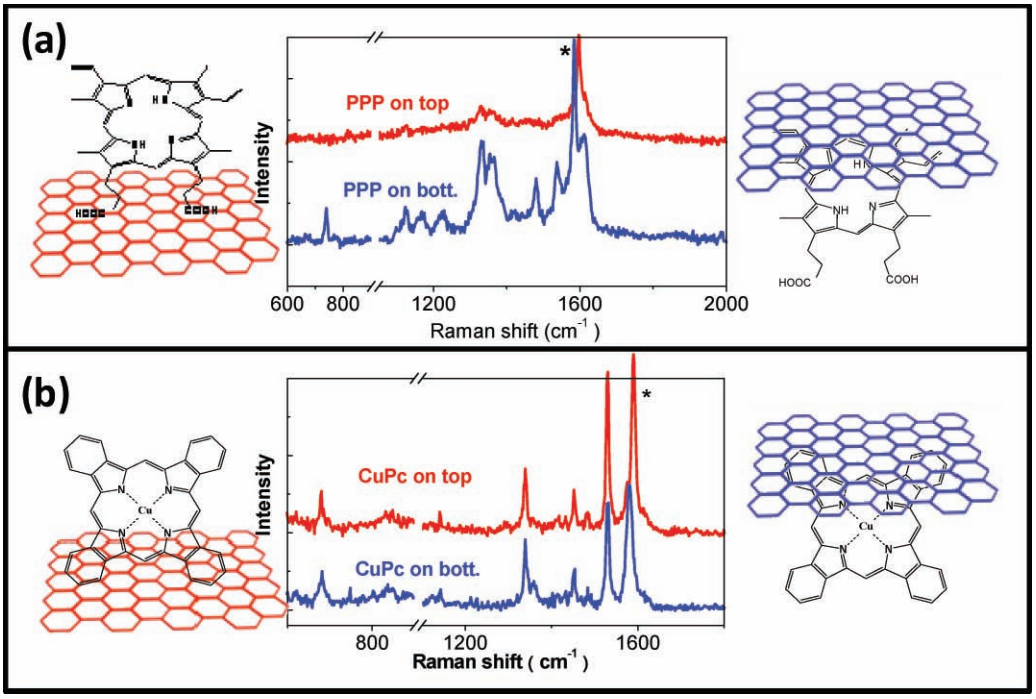

Figure 6. Raman spectra of PPP (a) and CuPc (b) on the top (red line) or the bottom (blue line) of graphene. The peaks labeled with "*" are the G-band from graphene. The insets in (a) and (b) show the corresponding molecular configuration on the top (left) or the bottom (right) of graphene.

NANO MICRO small

Table 1. Assignments of the peaks from PPP observed in our experiment. The inset shows the structure of PPP and the label of the carbon atoms.

Peak [cm^{-1}]	Assignment[32]	Assignment[33]
738	δ(Ca-N-Ca)	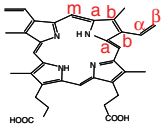
1123	IR: ν(Cb-Ca) RR: ν22 Ca-N	
1164	ν(Cb-Ca)	
1220	ν(Cb-Ca) δCm-H	29% Ca-Cb, 58% δCm-H
1330	δs(= CH_2)	38% Ca-Cb, 31% Ca-Cm, 17% Cb-Cb
1360		45% Ca-Cm, 37% Ca-N
1480	ν28Ca-Cm	57% Cb-Cb, 16% Ca-Cm
1537		
1606	ν(Cb-Cb)	

3. Conclusion

With the assistance of the LB technique, different layer numbers of LB films of PPP and different molecular configurations in contact with graphene have been fabricated. Based on one of the most important features of the chemical-enhanced mechanism in SERS, the first-layer effect was investigated in the GERS system. It was found that the first-layer LB film of PPP contributed the most to the Raman enhancement. Meanwhile, the closer the chemical group was to graphene, the stronger was the enhancement observed. All the results showed that the distance, which strongly influenced the degree of charge transfer between graphene and the molecule, played an important role in GERS. This is convincing evidence showing that GERS obeys the chemical-enhanced mechanism. This discovery provides a convenient system for the study of the chemical-enhanced mechanism and will benefit further understanding of SERS.

4. Experimental Section

PPP was purchased from Frontier Scientific, Inc., and used directly. The preparation and characterization of graphene were similar to those in our previous work.[22] The LB film of PPP was prepared as reported previously[31] in a LB trough (NIMA Technology, Type: 611, Serial No. 093). The monolayer was transferred onto a substrate in the upstroke mode and Z-type LB films were obtained.[31]

Raman spectra were collected on a Horiba HR800 Raman system with a 514.5 nm Ar^+ laser (Spectra-Physics model 163-C4205). A 100× objective was used to focus the laser beam. The laser power on the sample was controlled low at about 0.1 mW to avoid the heating effect and the decomposing of PPP. The spectra for comparison were obtained under the same conditions. The intensities of the peaks were obtained by fitting them with the Lorentzian function.

Supporting Information

Supporting Information is available from the Wiley Online Library or from the author.

Acknowledgements

This work was supported by NSFC (20673004, 20725307, 10774006, and 50821061), MOST (2006CB932701, 2006CB932403, 2007CB936203), and "the Fundamental Research Funds for the Central Universities."

[1] A. Campion, P. Kambhampati, *Chem. Soc. Rev.* **1998**, *27*, 241–250.
[2] M. Moskovits, *J. Raman Spectrosc.* **2005**, *36*, 485–496.
[3] A. Otto, I. Mrozek, H. Grabhorn, W. Akemann, *J. Phys. Condens. Matter* **1992**, *4*, 1143–1212.
[4] M. Fleischm, P. J. Hendra, A. J. Mcquilla, *Chem. Phys. Lett.* **1974**, *26*, 163–166.
[5] S. M. Nie, S. R. Emery, *Science* **1997**, *275*, 1102–1106.
[6] H. X. Xu, E. J. Bjerneld, M. Kall, L. Borjesson, *Phys. Rev. Lett.* **1999**, *83*, 4357–4360.
[7] R. K. Chang, T. E. Furtak, *Surface Enhanced Raman Scattering* Plenum, New York **1982**
[8] G. C. Schatz, M. A. Young, R. P. Van Duyne, *Surface-Enhanced Raman Scattering: Physics and Applications* **2006**, *103*, 19–45.
[9] B. N. J. Persson, K. Zhao, Z. Y. Zhang, *Phys. Rev. Lett.* **2006**, *97*, 199702.
[10] B. N. J. Persson, K. Zhao, Z. Y. Zhang, *Phys. Rev. Lett.* **2006**, *96*, 207401–207404.
[11] E. C. Le Ru, P. G. Etchegoin, *Phys. Rev. Lett.* **2006**, *97*, 199701.
[12] I. Mrozek, A. Otto, *Europhys. Lett.* **1990**, *11*, 243–248.
[13] I. Mrozek, A. Otto, *Appl. Phys. A Mater. Sci. Process.* **1989**, *49*, 389–391.
[14] A. Otto, *Top. Appl. Phys.* **1984**, *54*, 289–418.
[15] J. R. Lombardi, R. L. Birke, *J. Phys. Chem. C* **2008**, *112*, 5605–5617.
[16] I. Mrozek, A. Otto, *J. Electron Spectrosc. Relat. Phenom.* **1990**, *54*, 895–911.
[17] G. L. Eesley, *Phys. Lett. A* **1981**, *81*, 193–196.
[18] J. E. Rowe, C. V. Shank, D. A. Zwemer, C. A. Murray, *Phys. Rev. Lett.* **1980**, *44*, 1770–1773.
[19] I. Pockrand, A. Otto, *Solid State Commun.* **1980**, *35*, 861–865.
[20] R. Dornhaus, R. K. Chang, *Solid State Commun.* **1980**, *34*, 811–815.
[21] D. A. Zwemer, C. V. Shank, J. E. Rowe, *Chem. Phys. Lett.* **1980**, *73*, 201–204.
[22] X. Ling, L. M. Xie, Y. Fang, H. Xu, H. L. Zhang, J. Kong, M. S. Dresselhaus, J. Zhang, Z. F. Liu, *Nano Lett.* **2010**, *10*, 553–561.
[23] A. K. Geim, K. S. Novoselov, *Nat. Mater.* **2007**, *6*, 183–191.
[24] F. Guinea, B. Horovitz, P. Le Doussal, *Solid State Commun.* **2009**, *149*, 1140–1143.
[25] M. Bruna, S. Borini, *Appl. Phys. Lett.* **2009**, *94*, 031901.
[26] F. Rana, *IEEE Trans. Nanotechnol.* **2008**, *7*, 91–99.
[27] G. Goncalves, P. A. A. P. Marques, C. M. Granadeiro, H. I. S. Nogueira, M. K. Singh, J. Gracio, *Chem. Mater.* **2009**, *21*, 4796–4802.
[28] H. Abe, K. Manzel, W. Schulze, M. Moskovits, D. P. Dilella, *J. Chem. Phys.* **1981**, *74*, 792–797.
[29] C. A. Murray, D. L. Allara, *J. Chem. Phys.* **1982**, *76*, 1290–1303.
[30] B. Das, R. Voggu, C. S. Rout, C. N. R. Rao, *Chem. Commun.* **2008**, *41*, 5155–5157.
[31] C. Li, T. Imae, *Langmuir* **2003**, *19*, 779–784.
[32] S. Choi, T. G. Spiro, K. C. Langry, K. M. Smith, *J. Am. Chem. Soc.* **1982**, *104*, 4337–4344.
[33] P. Stein, J. M. Burke, T. G. Spiro, *J. Am. Chem. Soc.* **1975**, *97*, 2304–2305.
[34] K. Ogawa, H. Yonehara, C. J. Pac, *Langmuir* **1994**, *10*, 2068–2070.

Received: May 31, 2010
Published online: August 20, 2010